RSC Advances

ROYAL SOCIETY OF CHEMISTRY

www.rsc.org/advances

The decomposition of methanol on Au-Pt bimetallic clusters supported by a thin film of Al_2O_3/NiAl(100)

Y.-D. Li[1], T.-W. Liao[1], C. X. Wang[1,2], C.-S. Chao[1], T.-C. Hung[1], C.Y. Ho[1], M.-F. Luo[1,*], Yu-Ling Lai[3], Yao-Jane Hsu[3]

[1]*Department of Physics and Center for Nano Science and Technology, National Central University, 300 Jhongda Road, Jhongli 32001, Taiwan*

[2]*College of Physics Science and Technology, Yangzhou University, Yangzhou 225002, China*

[3]*National Synchrotron Radiation Research Center, 101 Hsin-Ann Road, Hsinchu Science Park, Hsinchu 30076, Taiwan*

*Corresponding author E-mail: mfl28@phy.ncu.edu.tw (M.F. Luo)

Keywords: Pt · Au · bimetallic clusters · Al_2O_3 · NiAl · Infrared reflection absorption spectra · Temperature-programmed desorption

Abstract

With various techniques to probe a surface, we studied the decomposition of methanol on Au-Pt bimetallic clusters, of diameter ≤ 6.0 nm, formed by sequential deposition of Au and Pt evaporated onto thin-film Al_2O_3/NiAl(100). The surface of the bimetallic clusters comprised both Au and Pt, but the decomposition, through dehydrogenation to CO and scission of the C-O bond, proceeded primarily on the surface Pt. Alloying of Pt with Au altered little the dehydrogenation on the Pt sites. The CO and hydrogen produced from dehydrogenated methanol increased with the extent of Pt sites; the production per surface Pt was comparable to that of Pt clusters. The temperature of the onset of dehydrogenation resembled that of Pt clusters. Little methanol decomposed to CO on the Au sites. Varying the surface structure and composition of the bimetallic clusters affected these properties insignificantly. In contrast to the dehydrogenation, scission of the C-O bond in methanol did not depend exclusively on the concentration of Pt atoms at the surface, given that production of methane from this second channel did not increase with the extent of Pt surface sites. The modified electronic structure of the alloyed Pt controlled the probability of the C-O bond scission. The bimetallic clusters restructured during the reaction such that the Au atoms in the clusters aggregated and decorated the Pt surface, leading to fewer surface Pt and increased mean coordination of surface Au.

Introduction

Platinum (Pt) catalysts to oxidize methanol (CH_3OH) have been extensively investigated because the principal reaction is applied in direct methanol fuel cells (DMFC), which generate electricity efficiently through the conversion of methanol,[1-5] but these Pt catalysts are easily poisoned by CO-like reaction intermediates. For the objective of diminishing the poisoning effect, the properties of supported Au-Pt bimetallic nanoclusters have been studied. The supported Au nanoclusters exhibited an exceptional catalytic reactivity for the oxidation of CO.[6,7] This alloying with Au is thus expected to suppress the poisoning, through either a bi-functional mechanism — methanol oxidation at Pt sites and CO oxidation at Au sites [8,9] — or synergistic effects that involve the variation of electronic band structures and lattice parameters.[10-13] Nevertheless, the effects of alloying on the principal reaction (decomposition of methanol) and the structural stability of the bimetallic clusters during the reaction remain unclear. These aspects determine the quality of the bimetallic clusters as practical catalysts. The aim of the present work is to reveal these properties with an ultrahigh-vacuum (UHV) model system.

We prepared the Au-Pt clusters by sequential deposition of Au and Pt (0.0 - 2.0 ML) evaporated onto a thin film of Al_2O_3/NiAl(100) at 300 K under UHV conditions. The morphologies and structures of the Au-Pt bimetallic clusters had been previously characterized with scanning tunneling microscopy (STM), reflection high-energy electron diffraction (RHEED), synchrotron-based photoelectron spectroscopy (PES), infrared reflection absorption spectroscopy (IRAS) and temperature-programmed desorption (TPD). The Au and Pt sequentially deposited on the Al_2O_3/NiAl(100) formed bimetallic clusters of diameter $\leq$ 6.0 nm and height $\leq$ 0.8 nm; they had a fcc phase and grew with their facets either (111) or (001) parallel to the θ-Al_2O_3(100) surface.[14,15] These bimetallic clusters had a mean lattice parameter about 4.2 Å, expanded about 7 % and 2 % with respect to bulk Pt and Au respectively.[14,15] The

electronic structures altered on alloying were reflected in the shifted binding energy (BE) of Au 4f and the evolving 5d derived states in the PES spectra.[14,15] Varied ratios (0.25 – 4) of Au to Pt in composition and alternate order of metal deposition yielded varied surface structures. The IRAS and TPD spectra of CO as a probe showed that, for the bimetallic clusters formed by deposition of Au onto Pt clusters (first Pt and then Au), the Au decorated preferentially and then aggregated the edge sites of Pt clusters, leaving a large uncovered Pt surface; for clusters formed in the reverse order of metal deposition, the Pt covered uniformly the surface of the existing Au clusters, so that the surface Pt sites increased and the Au sites decreased as Pt was deposited.[16]

The reactions of methanol (and also methanol-d_4) on the Au-Pt bimetallic clusters were monitored primarily with IRAS and TPD spectra. The results show that the alloying of Pt with Au altered little the dehydrogenation of methanol on Pt. The dehydrogenation occurred primarily on Pt sites of the bimetallic clusters; as on Pt clusters,[17] the process was initiated about 150 K and completed about 350 K. The average quantities of CO and hydrogen produced per surface Pt on the bimetallic clusters were similar to those on Pt clusters.[17] These properties were retained for varied surface composition and structures of the bimetallic clusters. The electronic structures of Pt modified on alloying and the Au-Pt intermixed surface sites affected little the dehydrogenation on Pt. Unlike the dehydrogenation, the scission of the C-O bond in methanol altered with the alloying. The methane produced did not increase simply with the surface Pt, despite this channel being open only when Pt existed on the surface. The scission of the C-O bond was governed by both the surface Pt sites and the modified electronic structures.

The surface structure of the bimetallic clusters became unstable as a result of the reactions. When adsorbed methanol decomposed, the surface Au aggregated and the extent of Pt on the surface decreased. This observation is consistent with a previous report[18] that adsorbed methanol drove Au to aggregate on Au-Pt bimetallic clusters. The restructuring is

attributed to adsorbed methanol and its reactions, rather than to the CO produced, as adsorbed CO was expected instead to increase the surface Pt.[19]

Experimental

Our experiments were performed in UHV chambers with a base pressure 4×10^{-10} torr. A NiAl(100) sample (MaTeck GmbH) was polished to a roughness less than 30 nm and an orientation accuracy better than 0.1°. To obtain a clean surface, the sample underwent alternative cycles of sputtering and subsequent annealing before each experiment. The cleanliness of the sample was monitored with Auger electron spectroscopy, low-energy electron diffraction and STM. An ultra-thin θ-Al_2O_3 film was formed on oxidation of a NiAl(100) alloy surface at 1000 K; the formation of Al_2O_3 thin films is described elsewhere.[20-23] To achieve a homogeneous crystalline Al_2O_3 surface with no NiAl facets, we refrained from protracted post-oxidation annealing of the oxide films.[23,24] The content of amorphous oxide surface was negligible[23] and the grown θ-Al_2O_3 thin film had thickness 0.5 – 1.0 nm.[20,23] The sample was then quenched to 300 K for vapor deposition of Pt and Au from ultra-pure Pt and Au rods heated by electron bombardment in commercial evaporators (Omicron EFM 3). The rate of deposition of metal was fixed about 0.1 monolayer (ML)/min, calculated according to the coverage prepared at 300 K. The coverage was estimated from the volume of the Pt (or Au) clusters observed with STM; 1 ML corresponds to density $1.5 \cdot 10^{15}$ (1.4×10^{15}) atoms/cm^2 of fcc Pt(111) (Au(111)) surface atoms.[25,26] After the deposition, the sample was cooled to the desired adsorption temperature (100 K, unless specified). Methanol or methanol-d_4 gas was dosed by a doser pointing to the sample, with a background pressure $2 – 5 \times 10^{-9}$ Torr. The methanol and methanol-d_4 (Merck, purity 99.8 %) were additionally purified by repeated freeze-pump-thaw cycles. We report methanol exposures in Langmuir units: 1 L = 10^{-6} Torr · s.

TPD spectra were taken by ramping the sample at 3 K/s and monitoring the various masses on a quadruple mass spectrometer (Hiden), which was shielded and placed close (about 2 mm) to the sample. IRAS spectra were collected using a Fourier transform infrared spectrometer (FTLA 2000) with external optics aligned for an incident angle 75° from the sample normal, and a liquid nitrogen-cooled HgCdTe detector. The IRAS spectra are presented as a ratio of data of sample and oxide surface (or clusters) measured at the same surface temperature (100 K), and are typically the average of 256 scans at resolution 4 cm^{-1}. The PES experiments were performed at beamline U5-spectroscopy at National Synchrotron Radiation Research Center in Taiwan.[27] The total energy resolution, including the beamline and energy analyzer, was estimated to be near 0.1 eV; the photon energies were fixed at 383 eV. The beam was incident normal to the surface; photoelectrons were collected at angle 58° from the surface normal. All photoelectron spectra presented here were first normalized to the photon flux. The BE is referred to the substrate bulk Al 2p core-level at 72.9 eV.[22,28,29]

Results and discussion

The Au-Pt bimetallic clusters were prepared by deposition of 0 – 2.0 ML of evaporated Au (or Pt) onto pre-deposited 1.0 ML Pt (or Au) on Al_2O_3/NiAl(100) at 300 K. Previous STM measurements showed that, for deposition of Au and Pt in either order, most subsequently deposited metal joined existing clusters when the coverage of the pre-deposited metal exceeded 0.5 ML.[14,15] Our sample preparation thus ensured that most grown clusters were bimetallic. The structural and morphological features of these bimetallic clusters on thin-film Al_2O_3/ NiAl(100) were examined with STM, IRAS and TPD, to ensure that the same features as those in preceding work (described above)[14-16] were retained.

1. Production of CO, D_2 and CD_4 from decomposed methanol-d_4

The reactions of both methanol and methanol-d_4 on the supported Au-Pt bimetallic clusters were characterized primarily with TPD and IRAS spectra. Comparison of the spectra from Pt clusters and the bimetallic clusters revealed the effect of alloying with Au. Adsorbed methanol and methanol-d_4 show the same thermal desorption behavior, but the signals of D_2 from methanol-d_4 were clearer than those of H_2 from methanol, due to their small background. Methanol-d_4 was hence used for the series of TPD experiments. We first compared the TPD spectra of CD_3OD, CD_2O, CO, D_2 and CD_4 from methanol-d_4 (CD_3OD) on 1.0 ML Pt clusters with those from Au-Pt bimetallic clusters formed by deposition of 1.0 ML Au onto 1.0 ML Pt clusters. The desorption of CD_3OD (top of Fig 1a,b) shows two distinct maxima, centered about 130 and 200 K. As the former feature never saturated and was observed on varied surfaces,[17,30-33] it is assigned primarily to desorption of multilayer methanol-d_4; the latter feature is ascribed to desorption of monolayer methanol-d_4 from Pt sites and the alumina film, as methanol on both Pt and alumina surfaces desorbs about 200 K.[17,33] The feature, centered about 130 K, of the bimetallic clusters (Fig. 1b) involved desorption of methanol-d_4 also from Au sites, as methanol-d_4 on Au sites desorbed near 150 K.[33] The cracking pattern of the desorbing methanol-d_4 dominated the CD_2O, CO and D_2 spectra in the same temperature regime (the second to fourth curves of Fig. 1a,b); the desorption of CO (150 – 200 K) and D_2 (100 – 150 K) from the Au sites[33] was negligible. Other than the cracking pattern of desorbing methanol-d_4 in the CD_2O spectra, no CD_2O signal was observed. A reaction path though formaldehyde as an intermediate is excluded. The CD_4 signals (m/z = 20 u) in this low-temperature regime resulted largely from the background, as these signals also appeared for methanol-d_4 adsorbed on Al_2O_3/NiAl(100). According to earlier experiments on (1 × 1) Pt(110),[31,34] D_2O (also m/z = 20 u) from decomposed CD_3OD might desorb between 150 and 200 K, but was indistinguishable from the background in the present work.

The CO and D_2 signals indicated dehydrogenation of methanol; the CD_4 signals indicated

an alternative channel of decomposition -- scission of the C-O bond. As desorption of neither CO nor D_2 nor CD_4, except the methanol-cracking pattern and background, was observed for methanol-d_4 on Al_2O_3/NiAl(100),[17] the decomposition must have occurred on the clusters. The spectra of CO and D_2 from the Pt clusters and from the bimetallic clusters are similar — the produced CO desorbed between 350 and 600 K and D_2 between 270 and 600 K (Fig. 1a,b), and the similarity persisted for the Pt clusters decorated with varied quantities (0 – 2.0 ML) of Au (Fig. 1c,d). This similarity indicates that the produced CO and D_2 desorbed primarily from the Pt sites or the Pt-alumina interface sites of the bimetallic clusters, and that the adsorption energies for CO and deuterium on the Pt alloyed with Au were little modified. The Pt sites of the bimetallic clusters, like those of Pt clusters, were the principal reaction sites. Although dehydrogenation might have occurred at the Au sites, the proportions of CO and deuterium produced there must be limited; the desorption features of produced CO and D_2 from Au were hardly observed.[33] With elevated temperature, the CO and D_2 might diffuse to the Pt sites to desorb, because the CO-Pt and D-Pt bonds are stronger.

The CO and D_2 spectra from the Pt clusters and from the Au-Pt bimetallic clusters differ in detail; these differences arise from their varied surface structures. With the incorporation of Au, the desorption of the produced CO decreased, and the desorption maximum shifted to a lower temperature (Fig. 1c). The spectrum altered because the deposited Au covered the Pt clusters and decorated preferentially the Pt sites of low coordination. As CO desorbs from low-coordinated Pt at a temperature higher than that from terrace Pt,[35-37] the fewer low-coordinated Pt sites resulted in a negative shift of the CO spectra. Similar desorption features were observed for CO molecularly adsorbed on the bimetallic clusters.[16] The electronic effect of alloying Pt with Au accounts little for this shift, because the same effect was not observed for bimetallic clusters with Pt uniformly on Au clusters (shown below and in Ref. 16). The CO desorption remained notably great even at 2.0 ML deposited Au (Fig. 1c), indicating that most Pt sites

were uncovered. This feature is consistent with a previous observation that aggregation of further deposited Au was favored at low-coordinated sites of Pt clusters, rather than covering uniformly the Pt surface.[16] The desorption of D_2 from the bimetallic clusters and the Pt clusters differs in the temperature regime between 270 and 400 K: there the D_2 desorption from the bimetallic clusters was quenched to a certain extent (indicated in Fig. 1b), which was observed at varied Au coverage (Fig. 1d). For Pt clusters, the desorption at 270 – 400 K was assigned to re-combinative desorption of D atoms from Pt sites, whereas at 400 – 600 K to desorption from the Pt-alumina interface.[17] Accordingly, the quenched desorption is likely associated with the fewer low-coordinated Pt sites.

The desorption of CD_4 indicated that decomposition occurred via scission of the C-O bond. As the adsorbed methanol (CH_3OH) yielded the same desorption of methane (CH_4) between 400 and 600 K (not shown), the observed signals at m/z = 20 u were from CD_4 rather than from D_2O. Our previous work showed that the scission of the C-O bond on Pt clusters occurred primarily in methanol itself and near 250 - 300 K; the intermediate methyl (CH_3) combined preferentially with atomic hydrogen from dehydrogenated methanol and desorbed as methane.[17] This process is expected to occur on the Pt sites of the bimetallic clusters, as scission of the C-O bond does not occur on Au clusters[33] and as the desorption of methane-d_4 from both the Pt and bimetallic clusters is similar, primarily between 350 and 600 K (Fig. 1a,b). Similar desorption features of methane-d_4 were observed for the bimetallic clusters formed with varied quantity of deposited Au. In common with the CO and D_2 signals, the intensity of the desorbing methane-d_4 decreased upon incorporation of Au into the clusters.

Figures 2a-c show the intensities of CO, D_2 and CD_4 desorption (from decomposed methanol-d_4 on the bimetallic clusters) as a function of the quantity of Au deposited on the 1.0 ML Pt clusters. For comparison, the desorption intensities of molecularly adsorbed CO at saturation on the Pt sites of the bimetallic clusters is plotted (red in Fig. 2a). 5 L CO was dosed

onto the sample at 100 K to achieve its saturation. The dashed lines in the figures indicate the desorption intensity of molecularly absorbed CO (red), and those of produced CO, D_2 and CD_4 from decomposed methanol-d_4 on 1.0 ML Pt clusters. With increasing deposition of Au, the desorption of molecularly adsorbed CO from the Pt sites (red) attenuated, as the Pt surface was gradually covered by Au atoms. The diffusion of adsorbed Pt from the interior to the surface of the bimetallic clusters, promoted by CO,[19] is limited in our system. Our preceding IRAS experiments with CO as a probe[16] indicated that the CO-promoted diffusion of Pt increased the intensity of the IRAS spectra from CO on Pt sites by only 10 - 20 %; besides, the CO signals from CO on Au sites differed little before and after the clusters restructured. The desorption intensity of molecularly adsorbed CO on Pt sites thus measured the number of Pt sites of the bimetallic clusters. The comparison of the desorption intensities of molecularly adsorbed CO and the produced CO (black) indicate that the quantity of produced CO varied in proportion to the number of Pt sites of the bimetallic clusters. This trend is consistently reflected in the quantity of the produced D_2 (Fig. 2b), which also decreased with the decreasing extent of Pt sites. The results support our argument that the dehydrogenation occurred primarily on the Pt sites of the bimetallic clusters. The quantity of produced CO amounted to about 70 - 80 % that of molecularly adsorbed CO at saturation: about 70 - 80 % of the original surface Pt sites were occupied by the produced CO. This value is slightly smaller than that observed on pure Pt clusters ($\geq$ 90 %). The produced D_2 exhibited a consistent picture, but the quantity of produced D_2 decreased more with the increased deposition of Au.

The intensity of the CD_4 TPD spectrum evolved with the deposited Au in a different manner. Upon depositing Au, the desorption intensity of CD_4 decreased, whereas, with further deposited Au, the intensity altered only little (Fig. 2c), in contrast with the systematically decreased desorption of the produced CO and D_2 (Fig. 2a,b). The quantity of produced CD_4 did not simply decrease with the decreased extent of Pt sites. The reason for the difference is

associated with a separate origin of the reactivity. The scission of the C-O bond of methanol on Pt single crystals was reported only on a (1 × 1) Pt (110) surface,[31,34] whereas the present Pt clusters lacked (110) facets. The reactivity toward scission of the C-O bond on Pt clusters is attributed to the nanometer size and the expanded lattice parameter of the clusters.[17] We discuss this behavior below with the data from the bimetallic clusters formed with Pt deposited on Au clusters.

The bimetallic clusters formed in the reverse order of metal deposition (first Au, then Pt) had a different surface structure. The deposited Pt covered uniformly the surface of existing Au clusters, leading to a structure more like Pt shell – Au core.[16] Methanol-d_4 decomposition on such bimetallic clusters gave results consistent with the above argument and also with their particular surface structures. Figure 3a shows the TPD spectra of CD_3OD, CD_2O, CO, D_2 and CD_4 for Au-Pt bimetallic clusters (formed on deposition of 1.0 ML Pt onto 1.0 ML $Au/Al_2O_3/NiAl(100)$) exposed to CD_3OD at 100 K. The cracking pattern of desorbing methanol-d_4 likewise contributed large CD_2O, CO, D_2 and CD_4 signals in the regime 100 - 250 K. Also no CD_2O signal was observed except the cracking pattern of desorbing methanol-d_4. The desorption temperatures for CO, D_2 and CD_4 from decomposed methanol-d_4 resembled those from Pt clusters; their desorption intensities increased with the extent of deposited Pt (Fig. 3b,c). These results confirm the dependence of the reactions on the Pt sites of the bimetallic clusters. The shape and position of the maximum in TPD spectra of the produced CO and D_2 were almost the same as those from Pt clusters, and remained unaltered with the Pt deposition (Fig. 3b,c). The shift of the maximum in the CO spectra and the quenching of the D_2 spectra (270 – 400 K) observed for the bimetallic clusters formed on deposition of Au onto Pt clusters were both absent. The same features of CO spectra were observed for CO molecularly adsorbed on bimetallic clusters of the same kind, showing that both terrace and low-coordinated Pt sites grew at a similar rate; the Au clusters were thus uniformly covered

with the deposited Pt.[16] The unquenched D_2 spectra between 270 and 400 K also implied a parallel growth of low-coordinated and terrace Pt sites. The alloying induced charge transfer from Pt to Au and also altered the 5d derived state (shown in the PES spectra[14,15]), but the modified electronic state of Pt affected little the adsorption energy of CO on Pt or the CO-Pt bonding. Our results indicate that the altered strength of the CO-Pt bond (on alloying with Au) observed from single crystals[11,38] or in an electro-oxidation environment[13] is not simply attributed to the formation of a Pt-Au bond: it is associated more with the complicated structural alteration around the surface Pt atoms after alloying.

Figures 4a-c show that the desorption intensities of the produced CO, D_2 and CD_4 varied with Pt deposited on 1.0 ML Au clusters/Al_2O_3/NiAl(100). With the desorption intensity of molecularly adsorbed CO on the Pt sites of the bimetallic clusters as a measure of the number of surface Pt sites (red in Fig. 4a), the produced CO and D_2 grew in proportion to the number of those Pt sites (Fig. 4a,b). Such a correlation is consistent with the above result that the Pt sites were the principal reactive sites for the dehydrogenation. In addition, the desorption signals of the produced CO and molecularly adsorbed CO that linearly increased with the deposited Pt (0.25 - 1.0 ML) verified that the deposited Pt covered the Au clusters, rather than forming three-dimensional Pt clusters. The produced CD_4 responded differently with the increased surface Pt. At 0.25 and 0.5 ML Pt, the produced CD_4 increased significantly, whereas above 0.5 ML Pt, the rate of increase declined despite the great increase of Pt sites (Fig. 4c). Like the result revealed in Fig. 2c, the scission of the C-O bond occurred when the Pt sites existed, but the probability of the scission did not depend exclusively on the number of Pt sites.

Figures 5a,b summarize the quantities of produced CO and D_2 (from TPD spectra) as a function of the surface Pt sites of pure Pt clusters (black) and bimetallic clusters (red and blue) formed in varied order of metal deposition. The number of surface Pt sites was measured also by the desorption intensity of molecularly adsorbed CO at saturation on the Pt sites. The

12

quantities of CO and D_2 produced per surface Pt on the bimetallic clusters formed with deposition of Pt on Au clusters (red) were comparable to those on pure Pt clusters, but those on the bimetallic clusters formed with deposition in the reverse order were slightly less (blue). As the numbers of monolayer methanol-d_4 on the pure Pt and the bimetallic clusters are expected to be similar, this comparison indicates that the probability of dehydrogenation of methanol-d_4 on the Pt sites of the bimetallic clusters was either comparable or slightly smaller. The probability was smaller on the bimetallic clusters formed with deposition of Au on Pt clusters (blue) because the deposited Au preferred to decorate the reactive Pt sites, which were low-coordinated Pt,[16] and that decreased the proportion of reactive Pt sites among all Pt sites.

In contrast with the dehydrogenation, the probability of scission of the C-O bond, reflected in the intensities of the CD_4 spectra, did not increase simply with the number of Pt sites (Fig. 2c and 4c). Figure 5c plots the intensities of the CD_4 TPD spectra as a function of the surface Pt sites of pure Pt clusters (black) and bimetallic clusters (blue and red) formed with deposition of metal in varied order. For the clusters formed with Au deposited on Pt clusters (blue), the CD_4 produced per surface Pt was generally less than that on Pt clusters; for the clusters formed with deposition in the reverse order (red), the production of CD_4 did not increase linearly with the Pt sites, unlike the behavior on Pt clusters (black). The Pt sites were thus not the only determining factor for the scission of the C-O bond in methanol-d_4. As the origin of reactivity for that scission was associated with the particular electronic structure of Pt clusters (because of the nanometer size and the expanded lattice parameter),[16] the electronic structure of Pt modified on alloying with Au played a role in the varied reactivity.

2. The activation energy of decomposition of methanol

The decomposition and the temperature dependence of the reaction were investigated with IRAS and PES. The spectra were recorded for methanol and methanol-d_4 adsorbed on the

bimetallic clusters at 100 K and annealed stepwise to selected temperatures. The characteristic evolution of the spectra with temperature for bimetallic clusters resembled that for Pt clusters, and depended little on the compositions of Au and Pt and the order of deposition of either metal. We present the following IRAS and PES spectra for the bimetallic clusters formed on deposition of 1.0 ML Au on 1.0 ML Pt clusters/Al_2O_3/NiAl(100) at 300 K as examples of the spectral features and the evolution. Figure 6a shows the IRAS spectra of C-O and C-D stretching modes for methanol-d_4 on the bimetallic clusters annealed to selected temperatures. The top line, for methanol-d_4 (3.0 L) on the sample at 100 K, has two absorption bands; one at 983 cm^{-1} is assigned to the C-O stretching (νCO) mode of methanol-d_4 and the other at 1128 cm^{-1} to the $\delta_s(CD_3)$ mode of methanol-d_4.[39-42] These wavenumbers differ little from those for methanol-d_4 on Al_2O_3/ NiAl(100) and Pt clusters. With increased temperature, the intensity of the C-O line decreased, and became zero about 300 K, because adsorbed methanol-d_4 either desorbed or decomposed. No sign of methoxy-d_4 was identified in this C-O stretching mode (expected to be 940 - 950 cm^{-1}),[39,41] indicating few methoxy-d_4 intermediates. Similar results were observed on Pt clusters.[17] The $\delta_s(CD_3)$ signals became small for monolayer methanol-d_4 (150 K) and almost vanished for sub-monolayer methanol-d_4 on the surface (200 K). The δ_sCD_3 absorption feature for methoxy, near 1100 cm^{-1},[39,41] was also undetectable.

Figure 6b shows the corresponding IRAS spectra for the O-D and other C-D absorption modes. The narrow absorption line at 2071 cm^{-1} and the asymmetric absorption centered about 2230 cm^{-1} are assigned to $\nu_s(CD_3)$ and $\nu_{as}(CD_3) + 2\delta_s(CD_3)$ of methanol-d_4, respectively;[39-42] the broad absorption centered near 2440 cm^{-1} is ascribed to the ν(OD) mode of methanol-d_4.[39,41] Consistent with the C-O stretching absorption, the intensities in the C-D and O-D regions decreased remarkably upon desorption of multilayer methanol-d_4 (upon annealing to 150 K). That the O-D absorption signals were absent at 150 K was due to the O-D stretching motion of the monolayer methanol-d_4 being nearly parallel to the surface, rather than to the

formation of methoxy. The O-D absorption was likewise not observed for monolayer methanol-d_4 on Al_2O_3/ NiAl(100). The C-D signals for the monolayer methanol-d_4 remained; their wavenumbers resembled those on Pt clusters or Al_2O_3/NiAl(100). On annealing to 200 K (for sub-monolayer methanol), the intensity of the $\nu_{as}(CD_3) + 2\delta_s(CD_3)$ mode approached the noise level and the wavenumber of the $\nu_s(CD_3)$ mode shifted to about 2082 cm^{-1}. The $\nu_s(CD_3)$ mode of methoxy, about 2050 - 2070 cm^{-1},[39-41] was never distinguishable. The shift of the $\nu_s(CD_3)$ mode to 2082 cm^{-1} is attributed to the incorporation of absorption signals of CO produced from dehydrogenated methanol-d_4 on the Au sites of the bimetallic clusters. The produced CO adsorbed on top of either low-coordinated Au or Au alloyed with Pt at 200 K.[16] Similar dehydrogenation of methanol on Au nanoclusters was previously observed.[33] With further elevated temperature, the produced CO desorbed or migrated to the vicinal Pt sites; this absorption feature hence vanished about 300 K (Fig. 6b). CO was unlikely to form on the Pt sites and to diffuse to the Au sites, because the CO-Pt bond is energetically preferable. The absorption line at 1947 cm^{-1} at 100 K is ascribed to contaminative CO co-adsorbed with methanol-d_4 on the Pt sites. The co-adsorption with methanol-d_4 decreased the wavenumber and intensity of the CO IRAS spectra.[17,33] With increased temperature, as the methanol-d_4 desorbed or decomposed to CO, relieving the co-adsorption effect, the CO line continued to grow and its wavenumber shifted to 2034 cm^{-1}.

To discern clearly the evolution of the CO IRAS, we recorded these spectra from dehydrogenated methanol on the bimetallic clusters formed with the same procedure (Fig. 6c). These spectra near 2070 cm^{-1} contained only CO signals. The top curve in Fig. 6c is from the bimetallic clusters before methanol adsorption, showing an absorption feature, about 2036 cm^{-1}, ascribed to contaminative CO on Pt sites. Upon adsorption of methanol, the CO feature broadened and shifted to 1963 cm^{-1} (the second curve in Fig. 6c), due to the co-adsorbed methanol. The same effect was mentioned above and seen previously for CO and methanol on

Au and Pt clusters.[17,33] On annealing to 150 K, as multilayer methanol desorbed and the effect of co-adsorbed methanol decreased, the CO line became restored to some extent: both the wavenumber and intensity increased. The effect of co-adsorbed methanol remained at 150 K, but the integrated intensity of the CO line became comparable to that from the contaminating CO, implying the onset of dehydrogenation of methanol to CO on the Pt sites. With further increased temperature, the CO signals from the Pt sites continued to increase because more methanol molecules were dehydrogenated to CO; at 350 K, the CO signals attained a maximum and the wavenumber increased to about 2038 cm^{-1}. Elevating further the temperature decreased the CO signals, as the CO desorbed. Figure 7 shows the CO signals from the Pt sites (relative to the CO contamination level) as a function of temperature, obtained from the bimetallic clusters formed with deposition of metal in either order (black and red). The error bars indicate the reproducibility, based on the results for 0.25 - 2.0 ML Au (Pt) deposited onto 1.0 ML Pt (Au) clusters. The trend is similar to that for Pt clusters.[17] As the contamination for the bimetallic clusters formed on deposition of Pt on Au clusters (red) was less than that with deposition in the reverse order (black), the produced CO from the former was evidently greater than the contaminative CO at 150 K. These results indicate that methanol on the bimetallic clusters was dehydrogenated to CO with an activation energy resembling that on Pt clusters; the possible intermediates were few. The dehydrogenation was sensitive to neither ensemble nor electronic effect introduced on allying.

The CO produced on the Au sites was also observed. The absorption line for CO on the Au sites, at 2083 cm^{-1} in Fig. 6c, became notable at 150 K and shifted to 2100 cm^{-1} at 200 K; above 250 K, the feature became indistinguishable as CO desorbed from the Au sites or migrated to the Pt sites. This observation corroborates the above result for methanol-d_4 on the clusters. No clear desorption feature of CO from the Au sites was observed in the TPD spectra, because the quantity of produced CO was small and also because the CO transferred to Pt sites to desorb.

16

The temperature dependence of scission of the C-O bond in methanol on the bimetallic clusters was revealed by PES spectra. Figure 8 shows PES from 1.0 L methanol adsorbed on the bimetallic clusters, formed on deposition of 1.0 ML Au on 1.0 ML Pt clusters/Al_2O_3/NiAl (100), and annealed to selected temperatures. The line initially centered about BE 287.8 eV was assigned to C 1s of methanol on the clusters,[43] the feature at 285.2 – 284.8 eV to C 1s of contaminative elemental carbon or CH_x. When the temperature was increased to 200 and 250 K, methanol desorbed or decomposed to CO; the remaining methanol and the produced CO gave a C 1s line shifted to 287.6 eV.[44] CO on the present Pt clusters gave C 1s signals near BE 287.5 eV, similar to that observed on Pt clusters/CeO_2.[45] On annealing to 300 and 380 K, the C 1s line at 287.6 eV shifted positively to 288.2 eV. At that temperature, no methanol remained, and formation of neither formaldehyde nor methoxy was indicated by the IRAS spectra. Formaldehyde on Pt clusters desorbed at 250 K,[46,47] and the C 1s of methoxy was expected at a smaller BE.[44] The signals were attributed to the produced CO that interacted with the hydroxyl (-OH) group from the scission of the C-O bond in methanol. The C 1s signals therefore shifted to a BE near that for the carboxyl (-COOH) group.[48-50] This shift indicates that the scission of the C-O bond began about 300 K, near the temperature for Pt clusters.[17] The C 1s signals for CH_x (285.2 – 284.8 eV) increased concomitantly. We exclude a contribution from elemental carbon because CO dissociated into elemental carbon about 500 K on Pt clusters.[36]

3. Restructuring of the Au-Pt bimetallic clusters with the reactions

The surface structure of the bimetallic clusters altered during the reactions. This structural alteration was evident through the contrast of the CO IRAS obtained from Pt and the bimetallic clusters. On Pt clusters, as the CO produced from dehydrogenated methanol tilted (because of co-adsorbed atomic hydrogen) and occupied only partly the Pt sites,[17] the IRAS spectra of the produced CO differed from those of molecularly adsorbed CO at saturation. Figure 9a

exemplifies the difference. We annealed the adsorbed methanol to 350 K to obtain maximal production of CO (ref. 17 and also Fig. 7); the molecularly adsorbed CO was dosed at 100 K and annealed to 300 K (to activate diffusion and reorientation of the CO) to obtain the maximal CO IRAS signals[16] for comparison. The annealing temperature 300 K (instead of 350 K) was used as the onset of desorption of molecularly adsorbed CO is near 300 K.[16,17] The former gave an IRAS line (red) with smaller intensity or wavenumber than that given by the latter (black). Adsorbing CO molecularly on these produced CO-covered Pt clusters increased the CO signals and rendered the CO line almost the same as that from CO at saturation, demonstrated in our previous work.[17] This result indicates that further adsorbed CO filled the unoccupied Pt sites. On the bimetallic clusters, the IRAS spectra of the produced CO from dehydrogenated methanol on Pt sites differed in a similar manner from those of CO molecularly adsorbed on Pt sites at saturation (red and black curves in Fig. 9b,c). As described above, the difference implies that the produced CO tilted and that its coverage on Pt sites was smaller than that of molecularly adsorbed CO at saturation. However, exposing the produced CO-covered bimetallic clusters to molecular CO increased little the intensity and wavenumber of the CO lines. Figures 9d,e demonstrate that 5 L CO dosed to the bimetallic clusters covered with the produced CO (from 3 L CH_3OH) failed to alter the CO spectra. The corresponding TPD spectra (not shown) confirmed that the further dosed CO did not adsorb on the bimetallic clusters. This behavior contrasts that shown on Pt clusters. As the atomic hydrogen impeded ineffectively the adsorption of CO on Pt sites[17] and as the produced CO is less than the molecularly adsorbed CO at saturation (Fig. 2a, 4a), the contrast indicates that no unoccupied Pt sites were available for the further dosed CO on the bimetallic clusters after the reaction of adsorbed methanol (annealed to 350 K). The Pt sites of the bimetallic clusters decreased during the decomposition of methanol.

The structural modification was also reflected in the CO spectra from the Au sites. Figure

10 compares the IRAS spectra of molecularly adsorbed CO (at saturation) on the Au sites of the bimetallic clusters formed by 1.0 ML Au deposited on 1.0 ML Pt clusters before (Fig. 10a) and after (Fig. 10b) the decomposition of methanol. The spectrum for the bimetallic clusters exposed to 5.0 L CO at 100 K exhibited a sharp absorption line at 2106 cm^{-1}, and a broad line centered about 2060 cm^{-1}, ascribed to CO on Au and Pt sites respectively (Fig. 10a). The absorption peak of CO on the Pt sites was small and broad because the adsorbed CO had not its optimal conformation at this low temperature; on annealing to 300 K, the line grew and sharpened like those in Fig. 9b,c.[16] The IRAS spectrum for CO on the bimetallic clusters that had been exposed to methanol at 100 K and annealed to 350 K (for methanol decomposition) showed an evidently less intense absorption at 2098 cm^{-1} for CO on the Au sites (Fig. 10b). The CO signals about 2040 cm^{-1} originated from CO produced from decomposed methanol on the Pt sites; as seen in Fig. 9d and e, these signals did not increase after adsorption of CO. The decreased CO signals for CO on the Au sites were due primarily to an increased coordination of the CO-binding Au. Our previous work showed a strongly enhanced infrared absorption of CO on Au sites of Au-Pt bimetallic clusters, attributed to a local field effect depending on the coordination of CO-binding Au.[51-53] The effect on the change of the signals is much stronger than that introduced by the decreasing Au sites.[16] The observed decrease of CO signals thus arose from an attenuated enhancement effect — an increased coordination of the CO-binding Au. As CO adsorbed only on edge Au (low-coordinated Au) or alloyed Au (with Pt) at 100 K,[18,33,35,54-57] the increased mean coordination of the CO-binding Au implies that corner Au and isolated Au on terrace became step Au or alloyed Au on a terrace surface. We thus speculate that, on reaction, Au atoms in the bimetallic clusters preferred to aggregate and to decorate the Pt surface, leading to decreased Pt sites and structurally more compact clusters.

The reaction-driven structural modifications are not simply due to the formation of CO from decomposed methanol. Previous work indicated that CO on Au-Pt bimetallic clusters

might, with increased temperature, induce the migration of Pt from the interior to the surface of the clusters, because of a strong CO-Pt bond.[19] Such a process is limited in our case[16] and increases the surface Pt sites, so is inconsistent with our observations. The effect of annealing to 350 K (for the reaction) is minor, as the clusters were prepared at 300 K and as the segregation of Au from Pt and the migration of Au atoms to the surface of bimetallic clusters occurred at a much higher temperature.[14-16] The mechanism of the structural alteration is unclear but the structure of the cluster evolved toward an energetically preferable one — an Au shell–Pt core structure.[58,59] The restructuring could be locally driven by the latent heat released on the decomposition of methanol, as the decomposition is an activated exothermic reaction.

Conclusion

The decomposition of methanol (also methanol-d_4) on Au-Pt bimetallic clusters on thin-film Al_2O_3/NiAl (100) was investigated with various surface probe techniques. Evaporated Au and Pt (0.0 – 2.0 ML) were sequentially deposited onto Al_2O_3/NiAl(100) at 300 K to form bimetallic clusters. Methanol on the bimetallic clusters decomposed through dehydrogenation to CO and scission of the C-O bond; the reaction occurred primarily on surface Pt sites of the bimetallic clusters. The alloying of Pt with Au altered little, through either ensemble or electronic effect, the dehydrogenation on the Pt sites. The produced CO and hydrogen from dehydrogenated methanol increased in proportion to the Pt sites; their production per surface Pt resembled those on Pt clusters. The activation energy for the dehydrogenation of methanol, reflected in the onset and completion of the dehydrogenation, was also near that on Pt clusters. Little methanol decomposed to CO on the Au sites. These properties were independent of the surface structure and composition of the bimetallic clusters. In contrast with the dehydrogenation, the scission of the C-O bond in methanol did not depend exclusively on the number of Pt sites: the methane produced from the second channel did not

increase simply with the Pt sites. The modified electronic structure of the alloyed Pt altered the probability of scission of the C-O bond. The reaction also induced an altered structure of the bimetallic clusters. The Au atoms in the clusters aggregated and decorated the Pt surface, resulting in decreased surface Pt and an increased mean coordination number of surface Au.

Acknowledgement

National Science Council provided support (grants NSC-98-2112-M-008-015-MY2 and NSC-100-2112-M-008-010-MY3) for the work.

References

[1] A. Hamnett, Catal. Today, 1997, **38**, 445.

[2] K. R.Williams, G. T. Burstein, Catal. Today, 1997, **38**, 401.

[3] G. T. Burstein, C. J. Barnett, A. R. Kucernak, K. R. Williams, Catal. Today, 1997, **38**, 425.

[4] B. Beden, C. Lamy, J. R. Leger, Electrocatalytic Oxidation of Oxygenated Aliphatic Organic Compounds at Noble Metal Electrodes; J. O. M. Bockris, B. E. Conway, R. E. White, Eds.; Plenum Publishers, New York, 1992.

[5] J. R. Rostrup-Nielsen, R. Nielsen, Catal. Rev. — Sci. Eng., 2004, **46**, 247.

[6] M. Haruta, Catalysis Today, 1997, **36**, 153-166

[7] M. Valden, X. Lai, D. W. Goodman, Science, 1998, **281**, 1647 – 1650.

[8] Y. Luo, M. M. Maye, L. Han, J. Luo, C.-J. Zhong, Chem. Comm., 2001, 473.

[9] J. Luo, P. N. Njoki, Y. Lin, D. Mott, L. Wang, C.-J. Zhong, Langmuir, 2006, **22**, 2892.

[10] S. Mukerjee, J. McBreen, J. Electrochem. Soc., 1999, **146**, 600.

[11] M. Ø. Pedersen, S. Helveg, a. Ruban, I. Stensgaard, E. Lægsgaard, J. K. Nøskov, F. Besenbacher, Surf. Sci., 1999, **426**, 395.

[12] J. Zeng, J. Yang, J. Y. Lee, W. Zhou, J. Phys. Chem. B, 2006, **110**, 24606.

[13] J. Suntivich, Z. Xu, C. E. Carlton, J. Kim, B. Han, S. W. Lee, N. Bonnet, N. Marzari, L. F. Allard, H. A. Gasteiger, K. Hamad-Schifferli, Y. Sao-Horn, J. Am. Chem. Soc., 2013, **135**, 7985 – 7991.

[14] M. F. Luo, C. C. Wang, G. R. Hu, W. R. Lin, C. Y. Ho, Y. C. Lin, Y. J. Hsu, J. Phys. Chem. C, 2009, **113**, 21054.

[15] M. F. Luo, C. C. Wang, C. S. Chao, C. Y. Ho, C. T. Wang, W. R. Lin, Y. C. Lin, Y. L. Lai, Y. J. Hsu, Phys. Chem. Chem. Phys., 2011, **13**, 1531.

[16] Y. D. Li, T. C. Hong, T. W. Liao, M. F. Luo, Surf. Sci. 2013, **618**, 132-139.

[17] C.-S. Chao, Y.-D. Li, B.-W. Hsu, W.-R. Lin, H.-C. Hsu, T.-C. Hung, C.-C. Wang, M.-F. Luo, J. Phys. Chem. C, 2013, **117**, 5667.

[18] C.-Y. Ho, R. B. Patil, C.-C. Wang, C.-S. Chao, Y.-D. Li, H.-C. Hsu, M.-F. Luo, Y.-C. Lin, Y.-L. Lai, Y.-J. Hsu, Surf. Sci., 2012, **606**, 1173-1179.

[19] S. A. Tenney, J. S. Ratliff, C. C. Roberts, W. He, S. C. Ammal, A. Heyden, D. A. Chen, J. Phys. Chem. C, 2010, **114**, 21652.

[20] P. Gassmann, R. Franchy, H. Ibach, Surf. Sci., 1994, **319**, 95.

[21] R. Blum, D. Ahlbehrendt, H. Niehus, Surf. Sci., 1998, **396**, 176.

[22] V. Maurice, N. Frèmy, P. Marcus, Surf. Sci., 2005, **581**, 88.

[23] M. S. Zei, C. S. Lin, W. H. Wei, C. I. Chiang, M. F. Luo, Surf. Sci., 2006, **600**, 1942.

[24] M. F. Luo, C. I. Chiang, H. W. Shiu, S. D. Sartale, C. C. Kuo, Nanotechnol., 2006, **17**, 360.

[25] S.D. Sartale, H.W. Shiu, M.H. Ten, J.Y. Huang, and M.F. Luo, Surf. Sci., 2006, **600**, 4978.

[26] M. F. Luo, H. W. Shiu, M. H. Tien, S. D. Sartale, C. I. Chiang, Y. C. Lin, Y. J. Hsu, Surf. Sci., 2008, **602**, 241.

[27] I.-H. Hong, T.-H. Lee, G.-C. Yin, D.-H. Wei, J.-M. Juang, T.-E. Dann, R. Klauser, T. J. Chuang, C. T. Chen, K.-L. Tsang, Nucl. Instrum. Methods A, 2001, **467-468**, 905.

[28] J. F. Moulder, W. F. Stickle, P. E. Sobol, K. D. Bomben, *Handbook of X-ray Photoelectron*

Spectroscopy, Physical Electronics, Inc. USA, 1995.

[29] S. D. Sartale, H. W. Shiu, M. H. Tien, C. I. Chiang, M. F. Luo, Y. C. Lin, Y. J. Hsu, J. Phys. Chem. C, 2008, **112**, 2066.

[30] B. A. Sexton, Surf. Sci., 1981, **102**, 271.

[31] J. Wang, R. I. Masel, J. Am. Chem. Soc., 1991, **113**, 5850.

[32] N. Kizhakevariam, E. M. Stuve, Surf. Sci., 1993, **286**, 246.

[33] G. R. Hu, C. S. Chao, H. W. Shiu, C. T. Wang, W. R. Lin, Y. J. Hsu, M. F. Luo, Phys. Chem. Chem. Phys., 2011, **13**, 3281.

[34] J. Wang, R. I. Masel, J. Vac. Sci. Technol. A, 1990, **9(3)**, 1879.

[35] D. C. Skelton, R. G. Tobin, D. K. Lambert, C. L. DiMaggio, G. B. Fisher, J. Phys. Chem. B, 1999, **103**, 946.

[36] Y.-N. Sun, Z.-H. Qin, M. Lewandowski, S. Shaikhutdinov, H.-J. Freund, Surf. Sci., 2009, **603**, 3099.

[37] M. J. Lundwall, S. M. McClure, D. W. Goodman, J. Phys. Chem. C, 2010, **114**, 7904.

[38] H. Ren, M. P. Humbert, C. A. Menning, J. G. Chen, Y. Shu, U. G. Singh, W.-C. Cheng, Appl. Catal. A: General, 2010, **375**, 303 – 309.

[39] J. S. Huberty, R. J. Madix, Suf. Sci., 1996, **360**, 144 - 156.

[40] W. S. Sim, P. Gardner, and D. A. King, J. Phys. Chem., 1995, **99**, 16002 - 16010.

[41] R. B. Barros, A. R. Garcia, L. M. Ilharco, J. Phys. Chem. B, 2001, **105**, 11186 - 11193.

[42] S. J. Pratt, D. K. Escott, D. A. King, J. Chem. Phys., 2003, **119**, 10867 – 10878.

[43] M. F. Luo, M. H. Ten, C. C. Wang, W. R. Lin, C. Y. Ho, B. W. Chang, C. T. Wang, Y. C. Lin and Y. J. Hsu, J. Phys. Chem. C, 2009, **113**, 12419-12426.

[44] I. Matolínová, V. Johánek, J. Myslivecek, K. C. Prince, T. Skála, M. Škoda, N. Tsud, M. Vorokhta, V. Matolín, Surf. Interface Anal., 2011, **43**, 1325.

[45] D. R. Mullins, K. Z. Zhang, Surf. Sci., 2002, **513**, 163.

[46] M. A. Henderson, G. E. Mitchell, J. M. White, Surf. Sci., 1987, **188**, 206.

[47] G. A. Attard, E. D. Ebert, R. Parsons, Surf. Sci., 1990, **240**, 125.

[48] S. H. Lee, T. Ishizaki, N. Saito, O. Takai, Surf. Sci.,2007, **601**, 4206.

[49] M. K. Kim, J. Baik, C. Jeon, I. Song, J. H. Nam, H.-N. Hwang, C. C. Hwang, S. H. Woo, C.-Y. Park, J. R. Ahn, *Surf, Sci.*,2010, **604**, 1598.

[50] M. S. Makowski, D. Y. Zemlyanov, J. A. Lindsey, J. C. Bernhard, E. M. Hagen, B. K. Chan, A. A. Petersohn, M. R. Medow, L. E. Wendel, D. Chen, J. M. Canter, A. Ivanisevi, Surf. Sci., 2011, **605**, 1466.

[51] R. G. Greenler, J. A. Dudek, D. E. Beck, Surf. Sci., 1984, **145**, L453.

[52] B. E. Hayden, K. Kretzschmar, A. M. Bradshaw, R. G. Greenler, Surf. Sci., 1985, **149**,394.

[53] T. Risse, A. Carlsson, M. Bäumer, T. Klüner, H.-J. Freund, Surf. Sci., 2003, **546**, L829.

[54] D. C. Meier, D. W. Goodman, J. Am. Chem. Soc., 2004, **126**, 1892.

[55] C. Lemire, R. Meyer, Sh. K. Shaikhutdinov, H.-J. Freund, Surf. Sci., 2004, **552**, 27.

[56] C. Winkler, A. J. Carew, S. Haq and R. Raval, Langmuir, 2003, **19**, 717.

[57] W. L. Yim, T. Nowitzki, M. Necke, H. Schnars, P. Nickut, J. Biener, M. M. Biener, V. Zielasek, K. Al-SHamery, T. Klüner and M. Bäumer, J. Phys. Chem. C, 2007, **111**, 445.

[58] R. Ferrando, J. Jellinek, R. L. Johnston, Chem. Rev., 2008, **108**, 847.

[59] H. B. Liu, U. Pal and J. A. Ascencio, J. Phys. Chem. C, 2008, **112**, 19173.

Captions of figures

Fig. 1 TPD spectra of CD_3OD (m/z = 36 u), CD_2O (m/z = 32 u), CO (m/z = 28 u), D_2 (m/z = 4 u) and CD_4 (m/z = 20 u) from 3.0 L CD_3OD adsorbed at 100 K on (a) 1.0 ML Pt clusters/Al_2O_3/NiAl(100) and (b) Au-Pt bimetallic clusters/Al_2O_3/NiAl(100) (formed with deposition of first 1.0 ML Pt and then 1.0 ML Au at 300 K); TPD spectra of (c) CO (m/z = 28 u)

and (d) D_2 (m/z = 4 u) from 3.0 L CD_3OD adsorbed at 100 K on Au-Pt bimetallic clusters formed on deposition of first 1.0 ML Pt and then varied quantities of Au (0.25 – 2.0 ML, as indicated in the figures) onto Al_2O_3/NiAl(100) at 300 K. The D_2 spectra are selectively presented because of significant overlapping among these spectra.

Fig. 2 Plots of integrated intensities of (a) CO, (b) D_2 and (c) CD_4 TPD spectra (from Au-Pt bimetallic clusters exposed to 3.0 L CD_3OD at 100 K) as a function of Au coverage. The Au-Pt bimetallic clusters formed on deposition of 0.25, 0.5, 1.0 and 2.0 ML Au onto 1.0 ML Pt/ Al_2O_3/NiAl(100) at 300 K. The red circles in (a) denote the integrated intensity of CO TPD spectra from the bimetallic clusters exposed to 5.0 L CO at 100 K. The dashed lines indicate the desorption intensity of molecularly adsorbed CO on 1.0 ML Pt clusters (red in (a)), and those of produced CO (black in (a)), D_2 (in (b)) and CD_4 (in (c)) from decomposed methanol-d_4 on 1.0 ML Pt clusters. The temperature ranges for the integrated signals are 350 – 600 K (CO), 270 – 650 K (D_2) and 350 - 650 K (CD_4). The error bars indicate the reproducibility and the fitting error.

Fig. 3 (a) TPD spectra of CD_3OD (m/z = 36 u), CD_2O (m/z = 32 u), CO (m/z = 28 u), D_2 (m/z = 4 u) and CD_4 (m/z = 20 u) from 3.0 L CD_3OD adsorbed at 100 K on Au-Pt bimetallic clusters formed on deposition of first 1.0 ML Au and then 1.0 ML Pt on Al_2O_3/NiAl(100) at 300 K; TPD spectra of (b) CO (m/z = 28 u) and (c) D_2 (m/z = 4 u) from 3.0 L CD_3OD adsorbed at 100 K on Au-Pt bimetallic clusters formed on deposition of first 1.0 ML Au and then varied quantities of Pt (as indicated in the figures) onto Al_2O_3/NiAl(100) at 300 K. The D_2 spectra are selectively presented because of significant overlapping among these spectra.

Fig. 4 Plots of integrated intensities of (a) CO, (b) D_2 and (c) CD_4 TPD spectra (from Au-Pt

bimetallic clusters exposed to 3.0 L CD_3OD at 100 K) as a function of Pt coverage. The Au-Pt bimetallic clusters were formed on deposition of 0.25, 0.5, 1.0 and 2.0 ML Pt onto 1.0 ML Au/ Al_2O_3/NiAl(100) at 300 K. The red circles in (a) denote the integrated intensity of CO TPD spectra from the bimetallic clusters exposed to 5.0 L CO at 100 K. The dashed lines indicate the desorption intensity of CO molecularly adsorbed on 1.0 ML Pt clusters (red in (a)), and those of produced CO (black in (a)), D_2 (in (b)) and CD_4 (in (c)) from decomposed methanol-d_4 on 1.0 ML Pt clusters. The temperatures ranges for the integrated signals are 350 – 600 K (CO), 270 – 650 K (D_2) and 350 - 650 K (CD_4). The error bars indicate the reproducibility and the fitting error.

Fig. 5 Plots of integrated intensities of (a) CO, (b) D_2 and (c) CD_4 TPD spectra from Pt (black circles) and Au-Pt bimetallic clusters as a function of surface Pt sites. The black circles indicate the data from Pt clusters at varied coverage (0.3, 0.4, 0.5, 1.0, 2.4 and 3.5 ML in (a), (b), and 0.3, 0.4 and 1.0 ML in (c)). The blue circles indicate the data from the bimetallic clusters prepared on deposition of first 1.0 ML Pt and then Au (0.25, 0.5, 1.0 and 2.0 ML) on Al_2O_3/NiAl(100) at 300 K; the red circles indicate those on deposition of first 1.0 ML Au and then Pt (0.25, 0.5, 1.0 and 2.0 ML). The numbers of the surface Pt sites were measured through the integrated intensities of TPD spectra of CO (5.0 L) as a probe. The dashed lines are drawn for visual guidance.

Fig. 6 IRAS spectra of (a) C-O, (b) O-D and C-D stretching modes for Au-Pt bimetallic clusters (formed on deposition of first 1.0 ML Pt and then 1.0 ML Au on Al_2O_3/NiAl(100) at 300 K) exposed to 3.0 L CD_3OD at 100 K and annealed to selected temperatures; (c) CO IRAS for the same sample exposed to 3.0 L CH_3OH at 100 K and annealed to selected temperatures.

26

Fig. 7 Plot of integrated intensities of CO IRAS spectra from dehydrogenated methanol on Au-Pt bimetallic clusters formed on deposition of Au on 1.0 ML Pt clusters (black squares) and on deposition of Pt on 1.0 ML Au clusters (red circles) on Al_2O_3/NiAl(100) at 300 K. The intensities are relative to those of contaminative CO; zero indicates that intensities are smaller than, or the same as, those of contaminative CO. The error bars indicate the reproducibility, based on the results of 0.25, 0.5, 1.0 and 2.0 ML Au (Pt) deposited onto 1.0 ML Pt (Au) clusters. The CO intensities obtained from any bimetallic clusters were normalized to the maximal one (350 K).

Fig. 8 C 1s photoelectron spectra from 1.0 L CH_3OH adsorbed on Au-Pt bimetallic clusters (formed on deposition of first 1.0 ML Pt and then 1.0 ML Au on Al_2O_3/NiAl(100) at 300 K) at 120 K and annealed to selected temperatures.

Fig. 9 (a) CO IRAS spectra for 1.0 ML Pt/Al_2O_3/NiAl(100) exposed to 3.0 L CH_3OH at 100 K and annealed to 350 K (red), and for the same sample exposed to 5.0 L CO at 100 K and annealed to 300 K (black); (b),(c) CO IRAS spectra for Au-Pt bimetallic clusters exposed to 3.0 L CH_3OH at 100 K and annealed to 350 K (red), and for the same sample exposed to 5.0 L CO at 100 K and annealed to 300 K (black); (d),(e) CO IRAS spectra for 3.0 L CH_3OH adsorbed on Au-Pt bimetallic clusters at 100 K and annealed to 350 K (the top), and subsequently exposed to 5.0 L CO at 100 K and annealed to 350 K (the bottom). The bimetallic clusters in (b) and (d) were formed on deposition of 1.0 ML Au onto 1.0 ML Pt/Al_2O_3/NiAl(100) at 300 K, and those in (c) and (e) on metal deposition in the reverse order.

Fig. 10 CO IRAS spectra for (a) 5.0 L CO adsorbed on Au-Pt bimetallic clusters (formed on deposition of 1.0 ML Au onto 1.0 ML Pt/Al_2O_3/NiAl(100) at 300 K) at 100 K, and for (b) the

same sample exposed to 3.0 L CH_3OH at 100 K, annealed to 350 K, and subsequently exposed to 5.0 L CO at 100 K.

28

Fig. 1

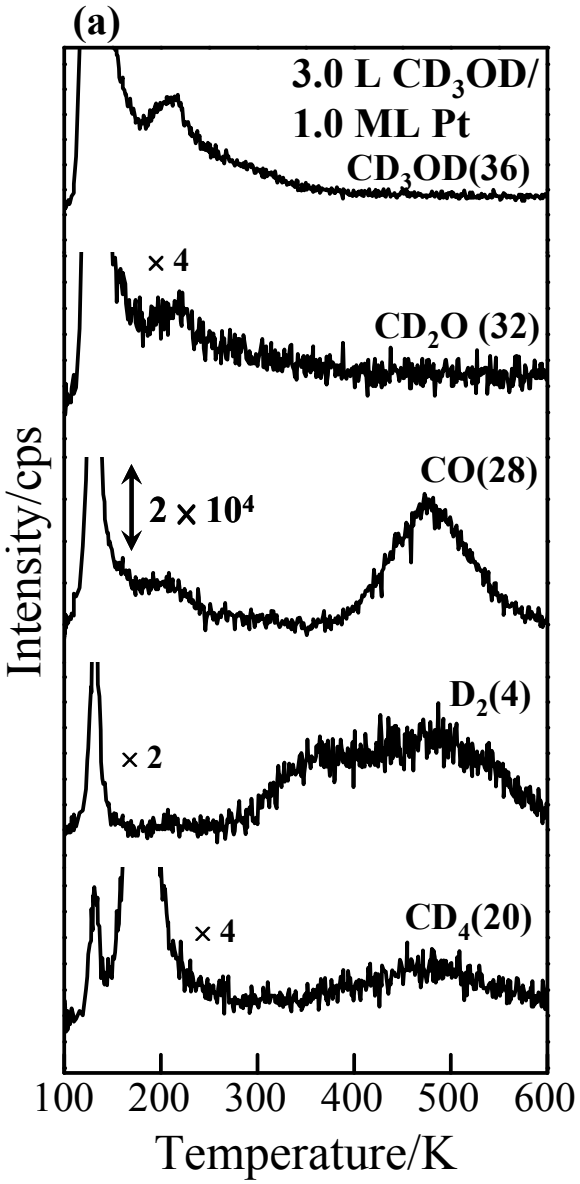

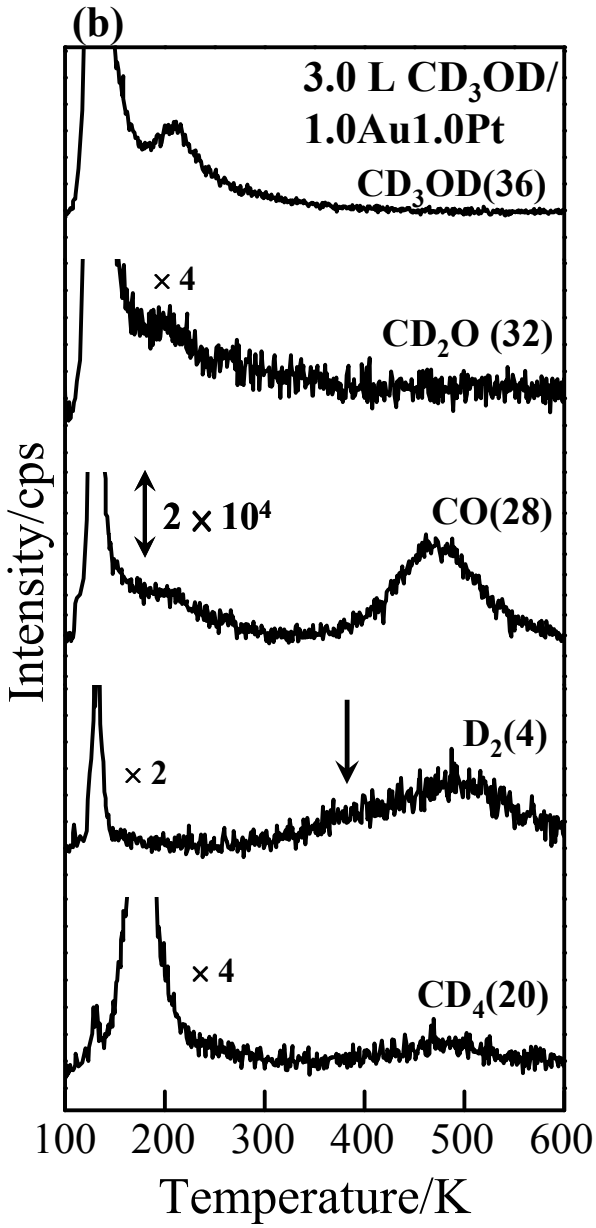

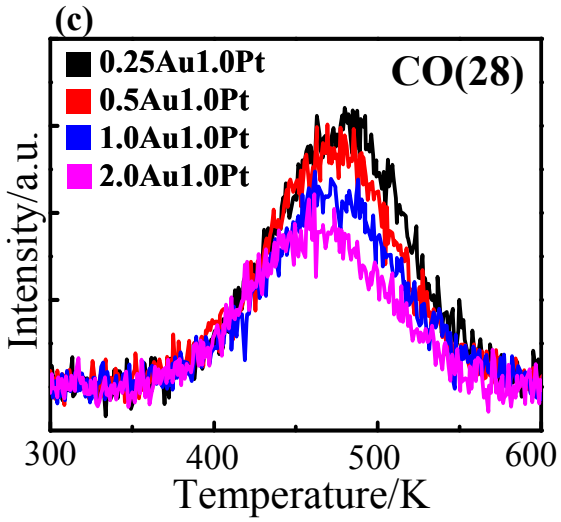

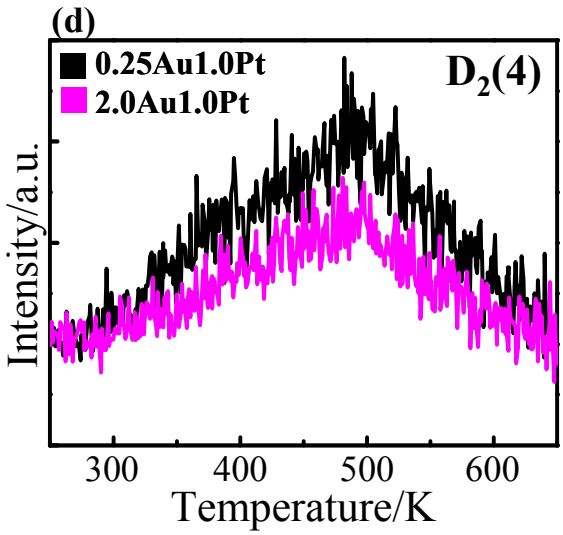

Fig. 2

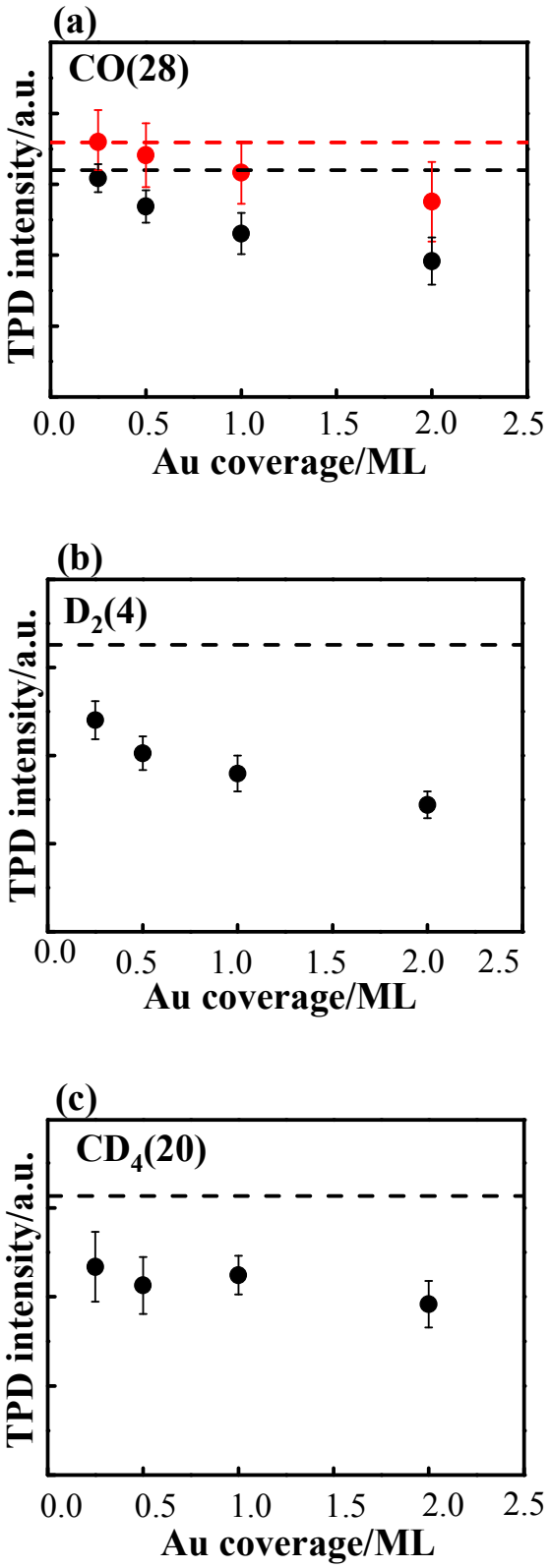

Fig. 3

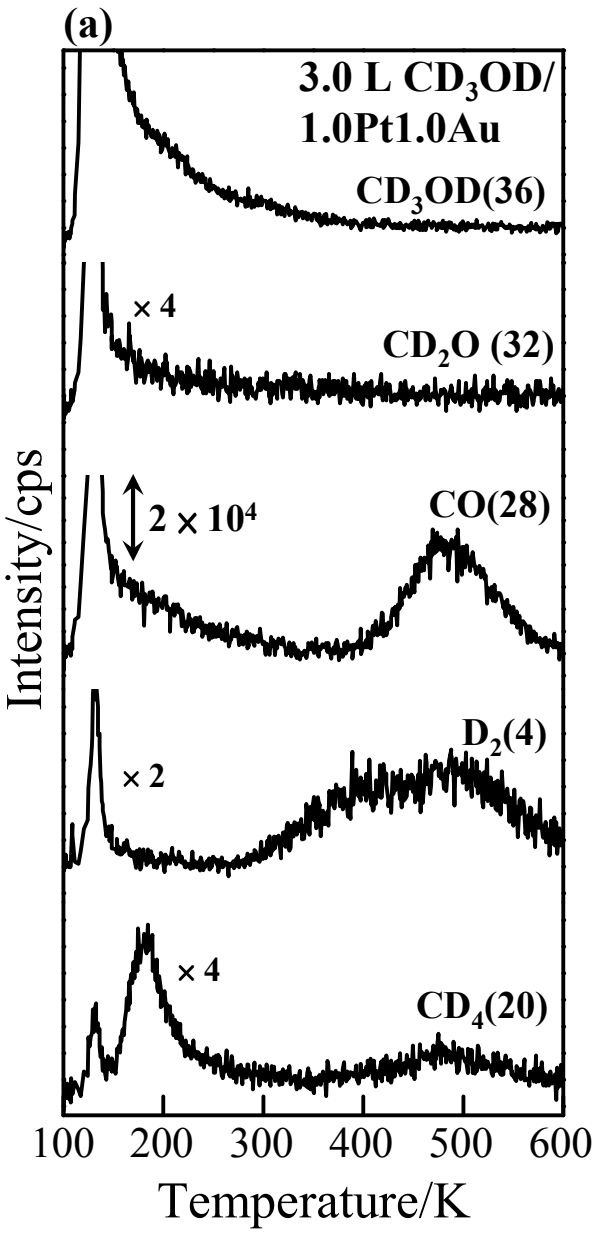

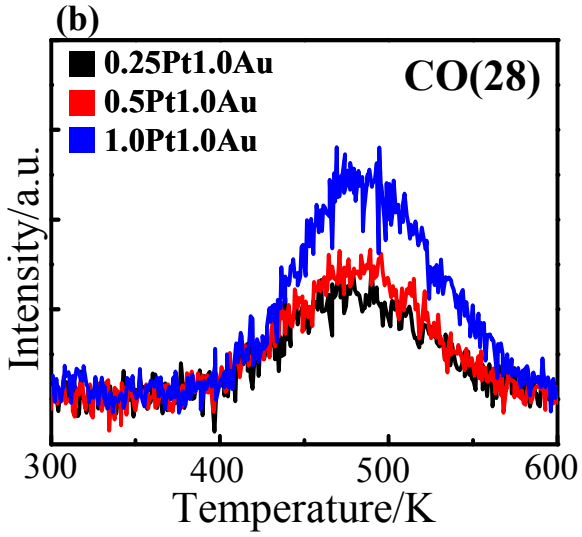

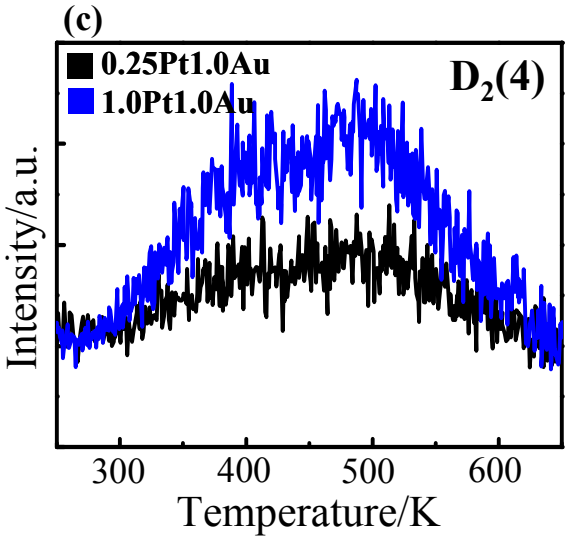

34

Fig. 4

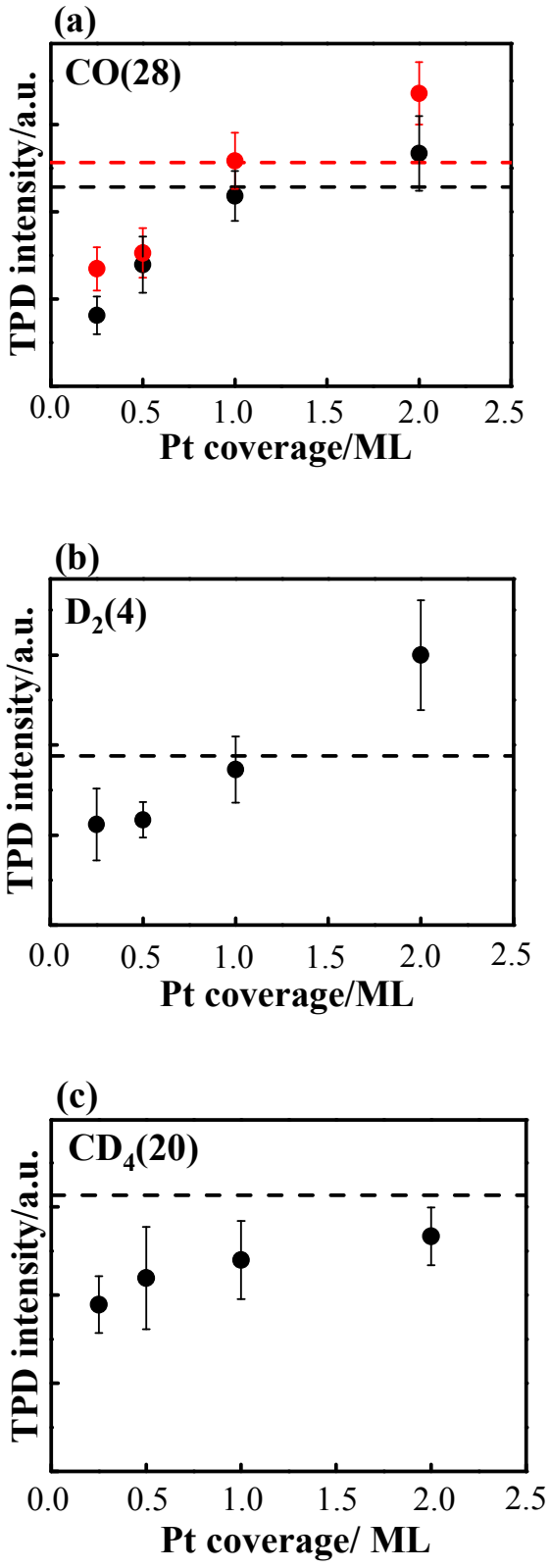

Fig. 5

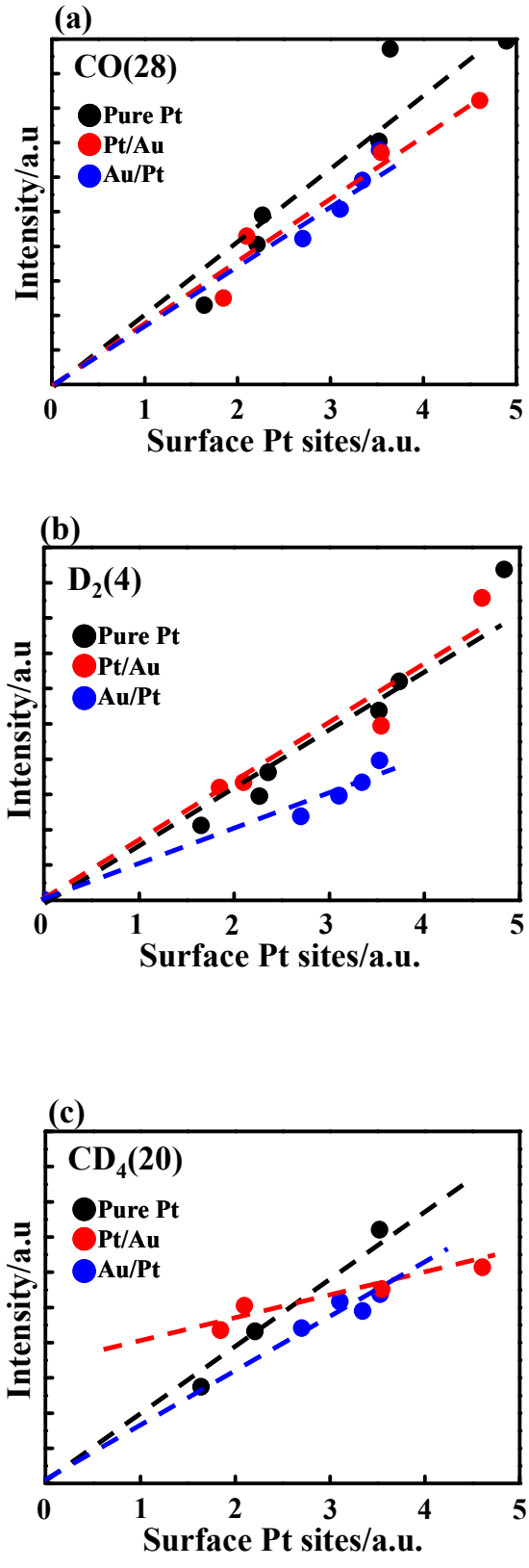

36

Fig. 6

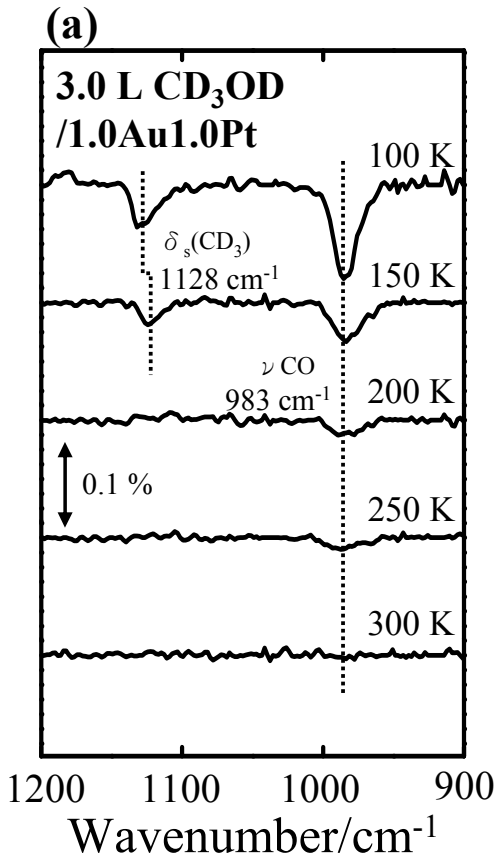

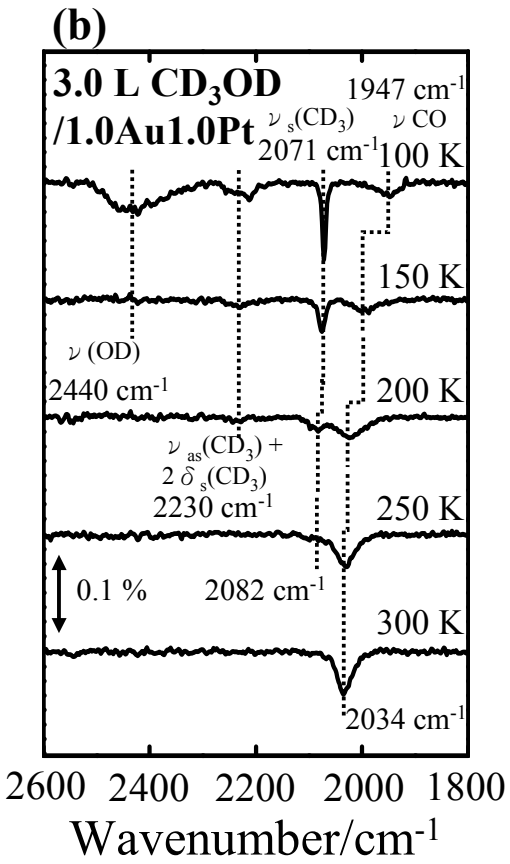

38

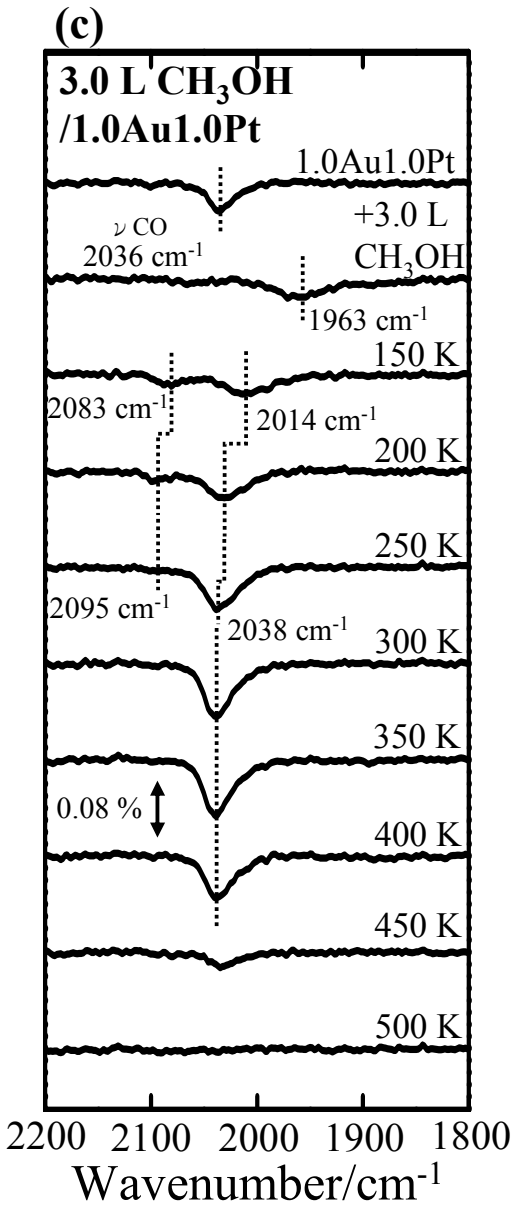

Fig. 7

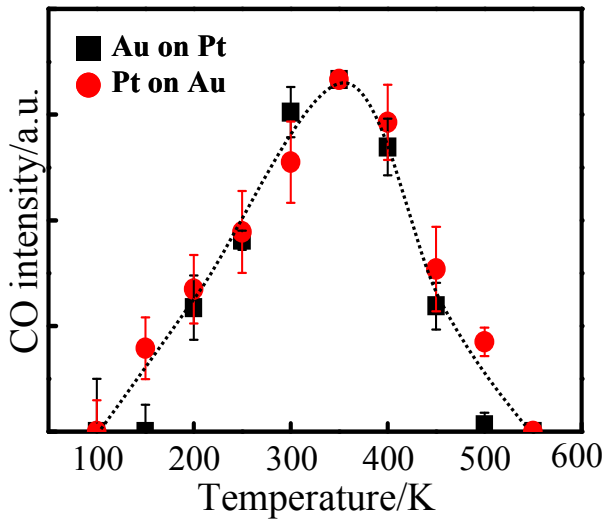

Fig. 8

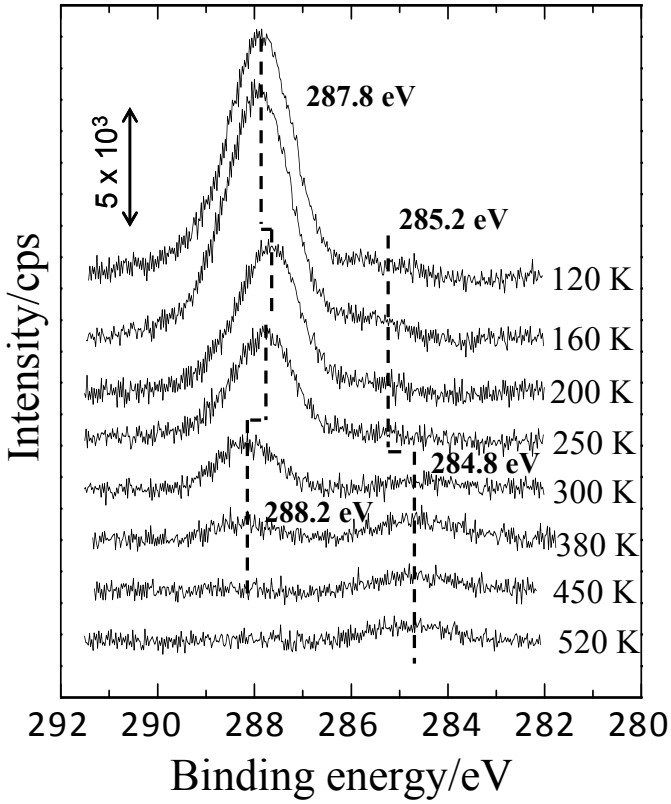

Fig. 9

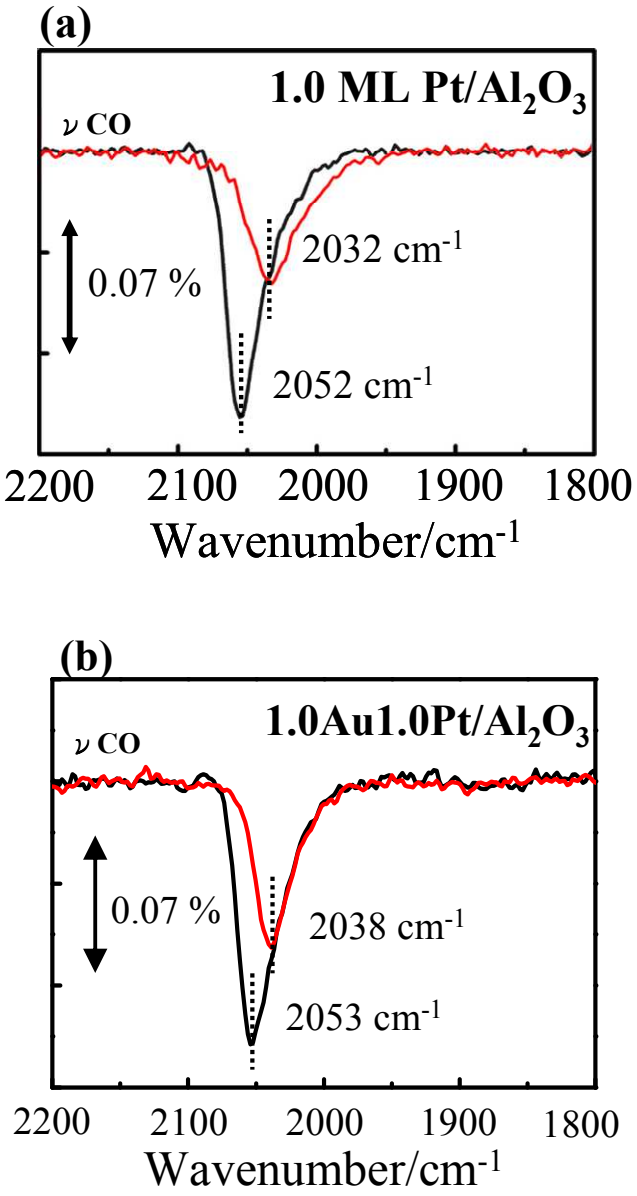

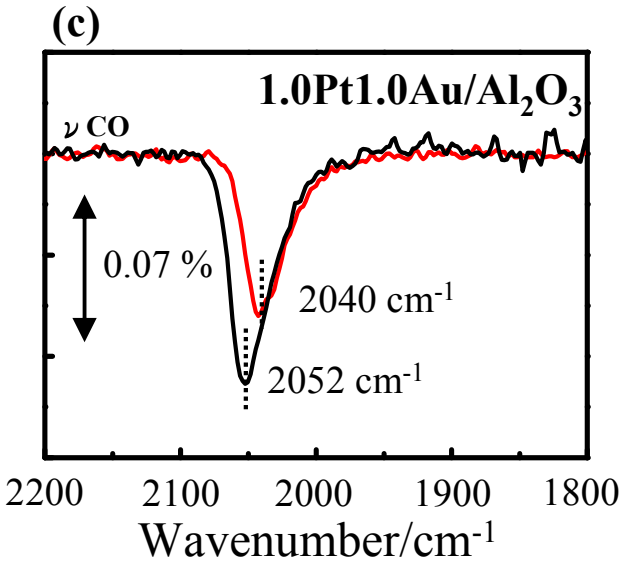

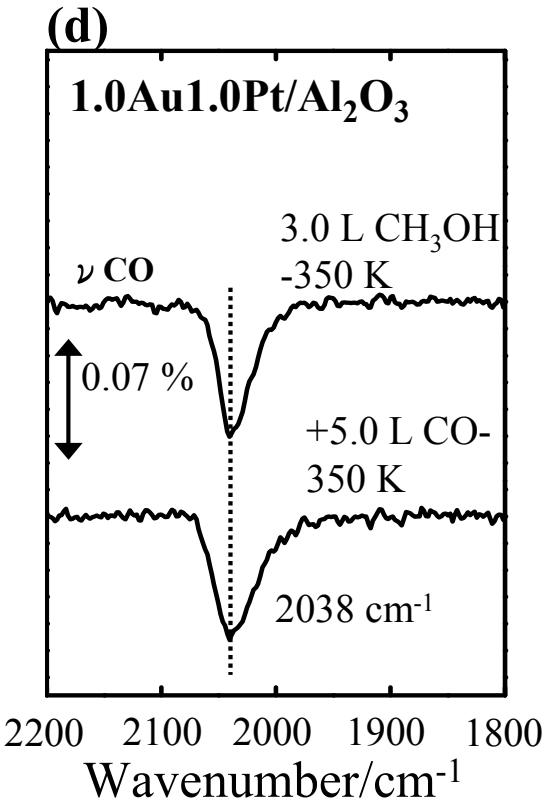

42

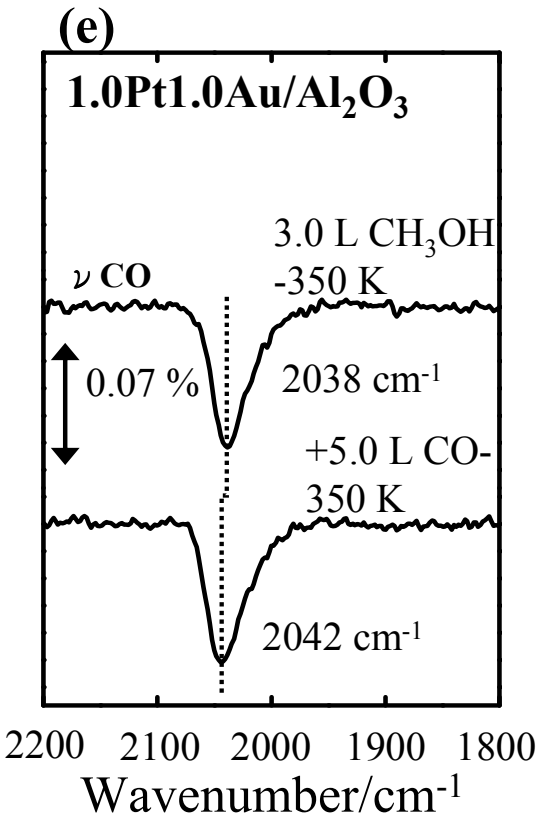

Fig. 10